



Changes in the flood plains and water quality along the Himalayan rivers after the Chamoli disaster of 7 February 2021

Sansar Raj Meena, Kushanav Bhuyan, Akshansha Chauhan & Ramesh P. Singh

To cite this article: Sansar Raj Meena, Kushanav Bhuyan, Akshansha Chauhan & Ramesh P. Singh (2021) Changes in the flood plains and water quality along the Himalayan rivers after the Chamoli disaster of 7 February 2021, International Journal of Remote Sensing, 42:18, 6984-7001, DOI: [10.1080/01431161.2021.1944696](https://doi.org/10.1080/01431161.2021.1944696)

To link to this article: <https://doi.org/10.1080/01431161.2021.1944696>



© 2021 The Author(s). Published by Informa UK Limited, trading as Taylor & Francis Group.



Published online: 17 Aug 2021.



Submit your article to this journal [↗](#)



Article views: 2814



View related articles [↗](#)







View Crossmark data [↗](#)



Citing articles: 8 View citing articles [↗](#)

Changes in the flood plains and water quality along the Himalayan rivers after the Chamoli disaster of 7 February 2021

Sansar Raj Meena ^{a,b,c}, Kushanav Bhuyan ^a, Akshansha Chauhan ^d
and Ramesh P. Singh ^e

^aFaculty of Geo-Information Science and Earth Observation (ITC), University of Twente, Enschede, The Netherlands; ^bDepartment of Geoinformatics—Z_GIS, University of Salzburg, Salzburg, Austria; ^cDepartment of Geosciences, University of Padua, Padua, Italy; ^dCenter for Space and Remote Sensing Research, National Central University, Taoyuan, Taiwan; ^eSchool of Life and Environmental Sciences, Schmid College of Science and Technology, Chapman University One University Drive, Orange, California, USA

ABSTRACT

The Himalayan regions are vulnerable to all kinds of natural hazards. On 7 February 2021, a deadly disaster occurred near the Tapovan, in Uttarakhand, Himalayas. During the event, large volume of debris along with broken glacial fragments flooded the Rishi Ganga River and washed away the nearby hydropower plants (Rishi Ganga and Tapovan), which was revealed from detailed analysis of multi spectral and bi-temporal satellite data. We present the impact of the Chamoli disaster on the flood plains and water quality of Himalayan rivers, Rishi Ganga near Tapovan, Alaknanda near Srinagar and Ganga near Haridwar and Bijnor. We used four locations along four sections of Himalayan rivers and have analysed various indices, modified normalized difference water index, normalized difference chlorophyll index, and normalized difference turbidity index, to study the changes in water quality and flood plains. On comparison of the spectral and backscattering coefficients derived from Sentinel-2 optical and Sentinel-1 synthetic aperture radar data, changes in the water quality and flood plains of the rivers were found.

ARTICLE HISTORY

Received 4 April 2021
Accepted 12 June 2021

1. Introduction

The glaciers in the higher Himalayas are the source of several rivers, which cross the Indo-Gangetic Plains (IGP). The dynamic nature of these rivers is controlled by the melting of glaciers and monsoonal precipitation. The sediments load in the rivers vary seasonally and yearly depending upon the meteorological parameters. Several small and large dams exist along the Himalayan rivers to regulate water levels, to protect from the floods and for power generation. New dams are being constructed and being planned for construction in the future (Tahbildar and Singh, 2005). The river waters are also connected with the long canals for irrigation purposes during poor

CONTACT Ramesh P. Singh  rsingh@chapman.edu  School of Life and Environmental Sciences, Schmid College of Science and Technology, Chapman University One University Drive, Orange, California, USA

© 2021 The Author(s). Published by Informa UK Limited, trading as Taylor & Francis Group.

This is an Open Access article distributed under the terms of the Creative Commons Attribution-NonCommercial-NoDerivatives License (<http://creativecommons.org/licenses/by-nc-nd/4.0/>), which permits non-commercial re-use, distribution, and reproduction in any medium, provided the original work is properly cited, and is not altered, transformed, or built upon in any way.

monsoon. The discharge of water from the Himalayan rivers is accumulated in large dam reservoirs Bhakra Nangal and Tehri dams in the Himalaya. Some of the large dams, which were built for longer life of more than 100 years, but due to fast erosion of young Himalayan mountains, the volume of sediments discharge has enhanced, thus, the dams have lost their capacity due to sediment depositions. The cleaning of sediment deposit in the reservoir suffers lack of cleaning facilities. The Himalayan region is prone to all kinds of natural hazards, such as earthquakes, snow avalanches, landslides, flash foods, landslide lake outburst foods (LLOFs), glacial lake outburst foods (GLOFs), rockslides, and debris flows (Ives 2004; Singh 2005a, 2005b; Bookhagen and Burbank 2010; Ziegler et al. 2014; Bhardwaj et al. 2021)

In the Himalayan region, frequent landslides induced from extreme precipitation and small earthquakes (Dash, Singh, and Voss 2000; Pradhan, Singh, and Buchroithner 2006; Roback et al. 2018; Gupta et al. 2019). Such landslides cause river damming (Fan et al. 2017), the flow of river gets affected due to blockage of rock mass and debris in the river, affecting the water quality. Along the rivers, many cities and villages are located, where the river water is the source for drinking, irrigation, washing and day to day works. The Ganga River water cross the IGP and the river water falls in the Bay of Bengal. The water quality of the river water and dynamics of the flow have strong seasonal characteristics associated with the change in meteorological parameters (rainfall, temperature), and construction activities, which sometimes induce rockslides causing volume of debris that block the water flow in the rivers (Paul et al. 2019; Peters, Meybeck, and Chapman 2005; Sun et al. 2016).

On 7 February 2021, Chamoli Glacial landslide caused huge rock falls and debris causing gushing volume of water in the river close to the source of the disaster. The inflow of the amount of water is still a mystery and scientists are making efforts to find the cause and source of huge volume of water flow. Large amount of water gushed in the Himalayan rivers, causing flash flood, change in the flood plains, and change in the water quality. The gates of dams were opened to allow water to flow to prevent flooding in the river close to the source and in the Ganga River. We have carried out analysis of satellite data near the source of the Chamoli event and along different sections of the Himalayan rivers, showing qualitative changes in the flood plains and water quality due to fall of rock mass and sediment debris.

The remote-sensing techniques are being used for monitoring water quality since the early 1970s (Ritchie, Zimba, and Everitt 2003). The spectral reflectance is widely used to monitor qualitative and quantitative water quality (Jupp et al., 1994)). The substances in the water can change the spectral characteristics of surface water, the wavelength characteristics are being used to monitor the type of organic sediments present in the water. With the advent of remote sensing, it is possible to detect these changes by assessing the spectral signatures from the water. The work reported by Ritchie, Zimba, and Everitt (2003) has clearly shown importance of remote-sensing data to map spatial and temporal variations in water quality parameters that are not easily or readily available from *in situ* data. Particularly, during disastrous events like flooding, where the possibility of site visits becomes dangerous, remote sensing offers a great alternative to assess information about the water quality. Furthermore, it promotes and encourages stakeholder participation to develop management plans for various natural resource and disaster management applications.

2. Chamoli disaster

On 7 February 2021, between 10:00 to 10:15 am (IST, local time), the disaster occurred; and the Rishi Ganga River was dammed and flooded due to the large amount of rockfall. As the landslide occurred, massive volume of water started flowing in the river that impacted the river flood plains. The satellite images clearly show the scar from where the glacier rock mass fell. Some of the ground and airborne photographs show fall of debris in the valley. Satellite images taken on 7 February 2021 at 05:01 am UTC and 7 February 2021 05:28 am UTC show dust in the valley (Meena et al. 2021a, 2021b) that was caused from the fall of glacial blocks and associated with the huge flow of water at the source. The sudden flow of huge amount of water washed out dams in the Chamoli area and took hundreds of lives. Soon after the disaster, the water appeared to be muddy near the origin (Meena et al. 2021a, 2021b), and with time, the quality of the river water considerably changed. In the present study, we have carried out analysis of flood plains and water quality using various indices based on optical data and comparing optical and SAR data along four sections of the Himalayan rivers. The water quality changed considerably over time depending upon the time of the disaster and muddy water reach at different sections in the river. We have analysed the pre-and post-Sentinel data to examine changes in water quality along four sections of the rivers (Figure 1): (1) Tapovan, (2) Srinagar, (3) Haridwar, and (4) Bijnor, all of which lie downstream from the source region. Along the Ganga River, location of Haridwar city is considered one of the religious locations, where Hindu religious people take a dip in river and plan all kinds of rituals and ceremonies in the river. Efforts have been made (Dwivedi, Mishra, and Tripathi 2018; Kamboj and Kamboj 2019) to monitor the quality of water since the river water is used for drinking purposes by people living along the river.

3. Data and methods

Sentinel-2 MSI level-1 C images were downloaded through Google Earth Engine's (GEE) open satellite image archive to investigate the water quality along the course of Ganga River and its tributaries (Gorelick et al. 2017). We have considered four locations to study the change in the water quality associated with the Chamoli disaster and the inadvertent effect of the sediment load in the river channels. We strategically chose locations near the disaster affected dam in the upper stream and sand bar areas on the flood plains in the lower stream areas to study the abrupt changes with the increase of large amount of water flow (by flooding) and increasing turbidity and chlorophyll concentrations along the rivers.

With the help of the GEE's JavaScript coding library, it was possible to address common issues of selecting and filtering of clouds-free optical and radar images for VV polarizations. We have used several indices and backscattering coefficient values for a qualitative assessment of the quality of water along the rivers and close to the disaster location.

Factors affecting water quality can change the surface signatures of water, among which suspended sediments, chlorophyll content, and others are easily detected with the indices. Flooding also has similar effects on water quality as it carries sediments and debris from the upper stream, increasing the turbidity of the flood plains. Moreover, by looking

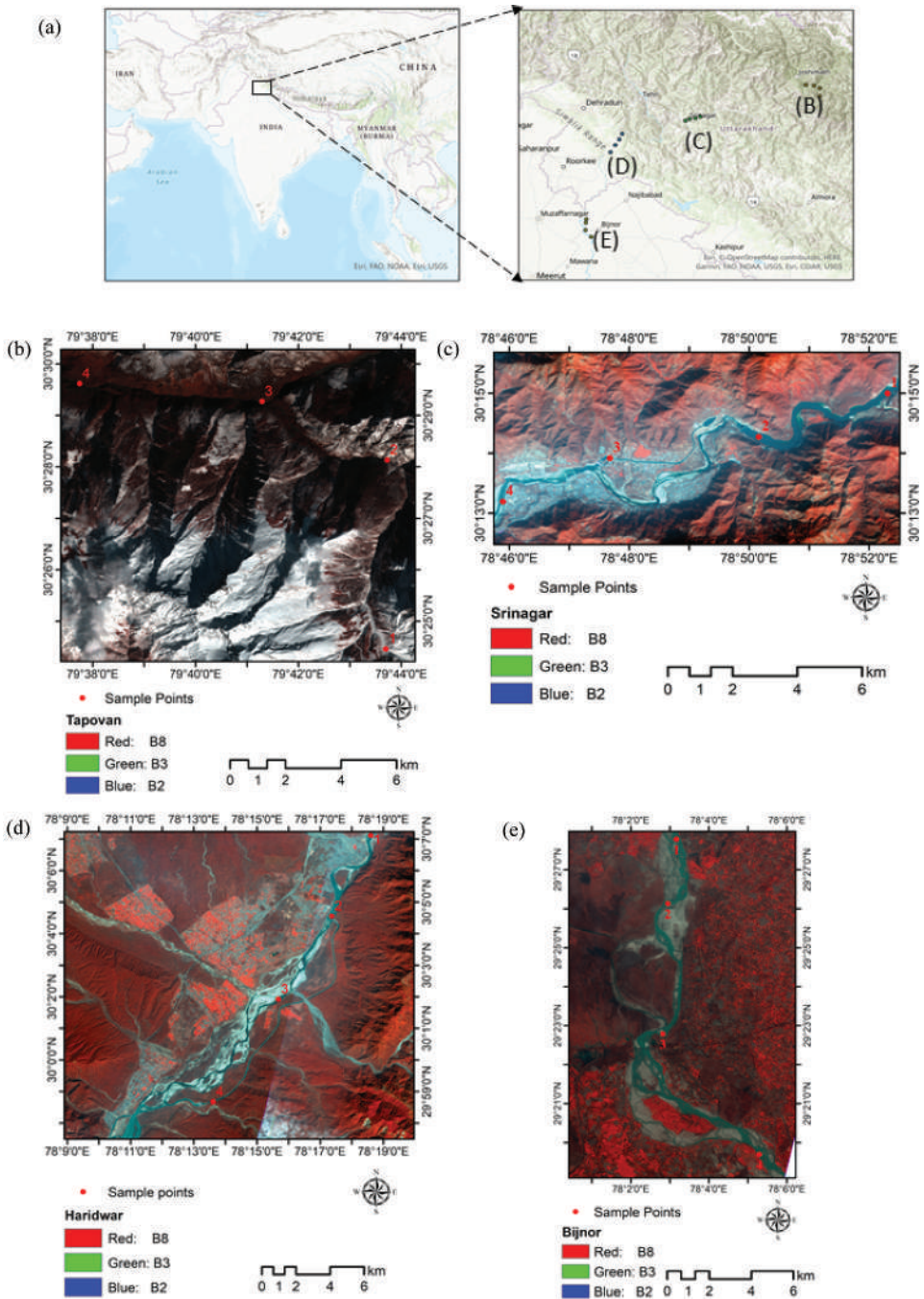


Figure 1. Study area locations: (a) overview of the study area; (b) Tapovan; (c) Srinagar; (d) Haridwar; and (e) Bijnor.

at river landscapes like sand bars, we can witness the changes in flood plains caused by increased water level. Hence, the use of these indices was employed in this research. The acquisition dates of the satellite images of Sentinel-1 and -2 are given in [Table 1](#).

3.1. Modified normalized difference water index (MNDWI)

Remote-sensing techniques provide the ease to analyse the changes over the earth surface. The mapping, monitoring, and dynamics of river water can be analysed using the spectral water index, various mathematical operations, ratios, differences, and normalized differences of two or more bands. Such arithmetic spectral operation also helps in cancelling out large portion of noise. The concept of the normalized difference water index (NDWI) was first developed by McFeeters 1996, which is defined as

$$NDWI = \frac{(R_G - R_{NIR})}{(R_G + R_{NIR})} \quad (1)$$

where R_G is the reflectance in green band (band 3 for Sentinel-2, [Table 2](#)) and

R_{NIR} is the reflectance in the near-infrared (band 8 for Sentinel-2, [Table 2](#))

The NDWI (Equation (1)) values greater than 0 indicates water cover and less than 0 indicates non-water surfaces, and also, a negative shift in NDWI is possible for muddy water or land region (Xu 2006). Based on trial-and-error method, we have found the threshold values for the water pixels. The NDWI normalized using a mid infrared (MIR) band instead of a NIR (near infrared) band enhances the detection of open water features and is found to be suitable for water bodies as it efficiently reduced noise from the background such as urban features (Xu 2006). Hence, in order to distinguish properly

Table 1. Information of image type (optical and SAR) and their respective dates.

Remote-sensing data	Image date
Optical image: Sentinel-2	5 February 2021 05:27 am UTC 10 February 2021 05:03 am UTC
SAR image: Sentinel-1 VV polarization	5 February 2021 10 February 2021

Table 2. Sentinel-2 image band information and their details.

Bands (wavelength region)	Central wavelength (nm)	Resolution (m)
Band – 1 (coastal aerosol)	443	60
Band – 2 (blue)	490	10
Band – 3 (green)	560	10
Band – 4 (red)	665	10
Band – 5 (vegetation red edge)	705	20
Band – 6 (vegetation red edge)	740	20
Band – 7 (vegetation red edge)	783	20
Band – 8 (NIR)	842	10
Band – 8A (vegetation red edge)	865	20
Band – 9 (water vapour)	945	60
Band – 10 (SWIR – Cirrus)	1375	60
Band – 11 (SWIR)	1610	20
Band – 12 (SWIR)	2190	20

between the sedimentation load and the existing water content in the river channels, we have considered modified NDWI normalized (Equation (2)) proposed by (Xu 2006).

$$MNDWI = \frac{(R_G - R_{SWIR})}{(R_G + R_{SWIR})} \quad (2)$$

where R_G is the reflectance in green band (band 3 for Sentinel-2, Table 2) and R_{SWIR} is the reflectance in the shortwave-infrared (band 8 for Sentinel-2, Table 2)

3.2. Normalized difference chlorophyll index (NDCI)

Chlorophyll concentration of the water depends on the level of nutrients in water along with the temperature. The flood water can change the chlorophyll concentration of the river. The NDCI is computed using Equation (3) (Mishra and Mishra 2012)

$$NDCI = \frac{(R_{VR} - R_R)}{(R_{VR} + R_R)} \quad (3)$$

where R_{VR} is the reflectance in vegetation red edge band (band 5 for Sentinel-2, Table 2) and

R_R is the reflectance in red band (band 4 for Sentinel-2, Table 2)

NDCI (Equation (3)) can be used to calculate the Chl-*a* concentration ($\mu\text{g L}^{-1}$) using following Equation (4)

$$Chl - a (\mu\text{g L}^{-1}) = 194.325 \times NDCI^2 + 86.115 \times NDCI + 14.039 \quad (4)$$

Higher values of NDCI reflect higher Chl-*a* and nutrient concentrations, which are considered as poor quality of water (USEPA 2008). The lower reference limit of Chl-*a* is $20 \mu\text{g L}^{-1}$ corresponds to 0.06 NDCI and higher NDCI values (>0.06) represent poor water quality as the Chl-*a* is greater than $20 \mu\text{g L}^{-1}$ (USEPA 2008). The negative NDCI values show the overflow conditions with lower Chl-*a* concentration.

3.3. Normalized difference turbidity index (NDTI)

The NDTI combines the red and green bands to classify the water quality. Water shows weak reflection in green, small in red and quasi-nell in near-infrared bands (Lacaux et al. 2007). The sedimentation in water affects the reflection due to the higher turbidity. The spectral information from the turbidity is similar to bare soils (Guyot 1989), and the reflection is higher in the red band compared to the green band. The radiometric calculation of NDTI is computed from the following Equation (5):

$$NDTI = \frac{(R_R - R_G)}{(R_R + R_G)} \quad (5)$$

where R_R is the reflectance in red band (band 4 for Sentinel-2, Table 2) and R_G is the reflectance in green band (band 3 for Sentinel-2, Table 2).

The positive values of NDTI indicate a higher level of turbidity, whereas the negative values indicate clean water. NDTI values vary in the range $(-0.03) - (0.03)$ are similar to those of arable land with a vegetation cover (Solovey 2019).

3.4. Sentinel-2 and Sentinel-1 derived information

The sensors on board the Sentinel-2 satellite measure the surface reflectance in different wavelengths (nanometres) (Table 2). The Sentinel-1 sensor sends out microwave signals that, upon touching the different land surfaces, get reflected as backscatter containing information about reflective strength (Perrou, Garioud, and Parcharidis 2018). The normalized measure of the radar return is known as the backscatter coefficient, defined per unit area on the ground (expressed in decibels) (Singha et al. 2020):

$$dB = 10 \cdot \text{Log}_{10} (\text{Energy Ratio}) \quad (6)$$

One of the essential features and advantage of radar is the microwave signals passing through gases and clouds, making it very suitable to detect water during monsoon periods that bring about thick cloud cover. The range of backscatter coefficient in different surfaces is given in Table 3.

4. Results and discussion

Various water quality indices derived from the Sentinel-2 optical data and Sentinel-1 synthetic aperture radar (SAR) data have been used to evaluate the changes in the Himalayan rivers water quality after the Chamoli disaster. Huge debris and glacial fragments were deposited into the Rishi Ganga River near Tapovan that affected the water quality and flood plains along the downstream rivers near Srinagar, Haridwar and Bijnor, thus affecting the changes in the flood plains (as seen in Figures 2 and 3) and water quality.

4.1. Changes in indices derived from Sentinel-2 data set

We analysed the changes in the water quality indices with the modified water index (MNDWI), turbidity (NDTI), and chlorophyll concentration (NDCI) at four locations (Table 4) in Tapovan, Srinagar, Haridwar and Bijnor. Our analysis is based on Sentinel-2 optical imageries before and after the Chamoli disaster.

Comparison of MNDWI index maps in Tapovan (Figure 4(a)) with Figure 4(b) show a drop in the MNDWI values, which can be attributed the presence of fresh snow particularly at two

Table 3. Backscatter coefficients range from Sentinel-1 (Stendardi et al. 2019).

Backscatter coefficients range	Different surfaces
Very high backscatter (above -5 dB)	<ul style="list-style-type: none"> ● Man-made objects (urban) ● Terrain slope towards the radar ● Very rough surfaces
High backscatter (-10 dB to 0 dB)	<ul style="list-style-type: none"> ● Steep radar angle ● Rough surfaces ● Dense vegetation (forest)
Moderate backscatter (-20 dB to -10 dB)	<ul style="list-style-type: none"> ● Medium level of vegetation ● Agricultural crops ● Moderately rough surfaces
Low backscatter (below -20 dB)	<ul style="list-style-type: none"> ● Smooth surfaces ● Calm water ● Roads ● Very dry soil (sand)

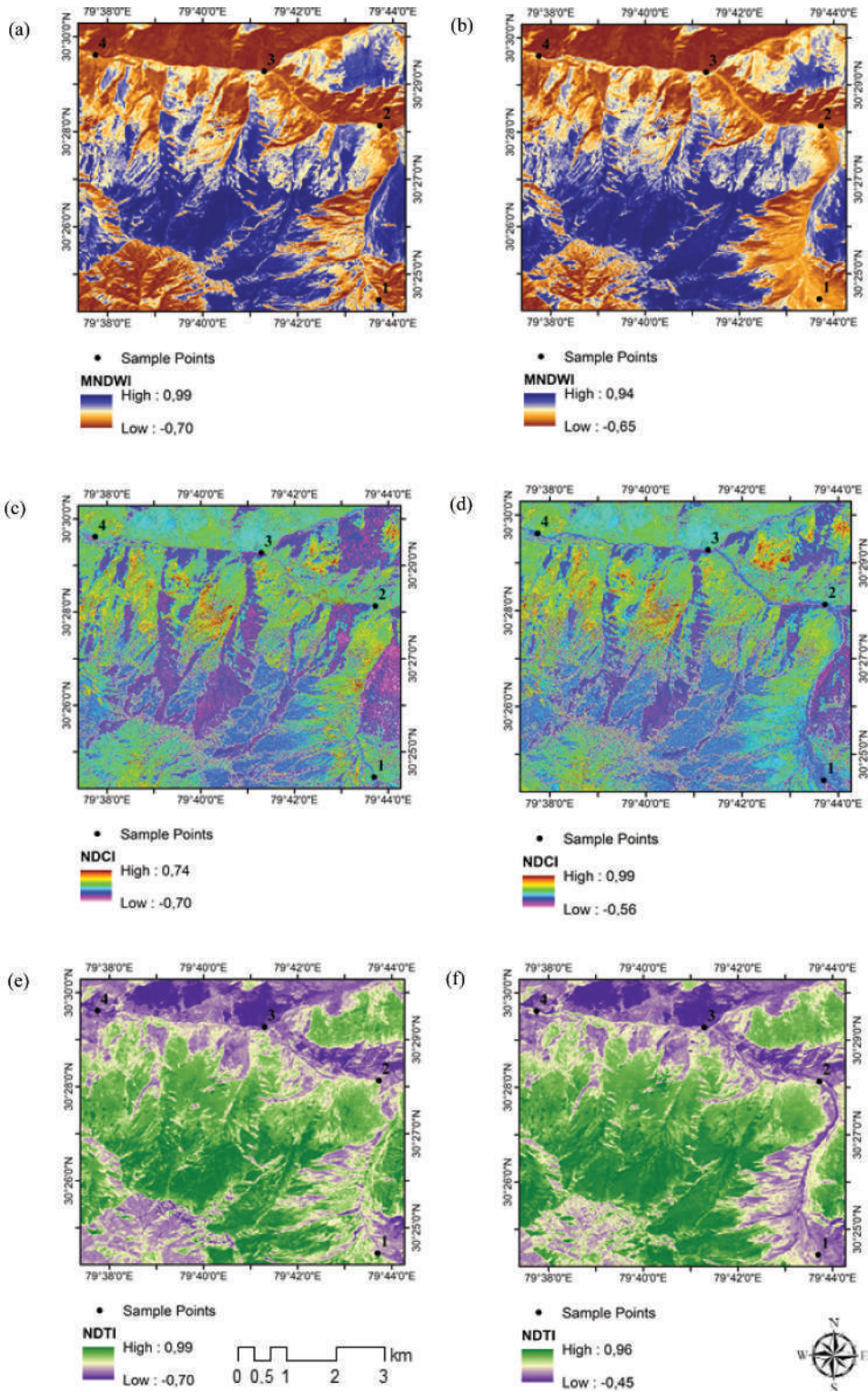


Figure 2. Changes in water quality indices and flood plains seen at four locations at Tapovan (a, c, e: pre-event and b, d, f: post-event).

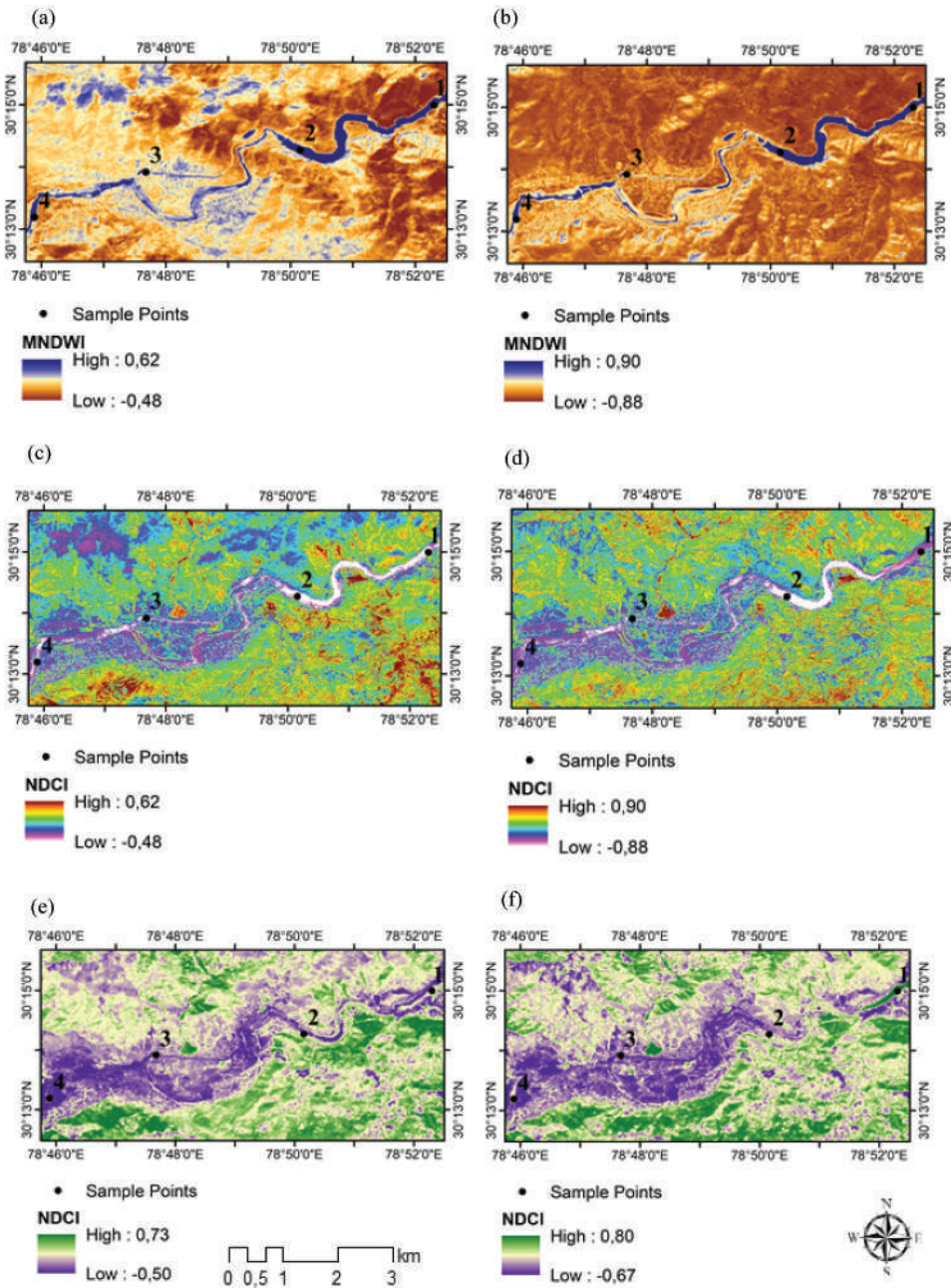


Figure 3. Changes in water quality indices at various locations for Srinagar (a, c, e: pre-event and b, d, f: post-event).

locations (points 1 and 2). The surface reflectance of snow or glacier ice is very low in SWIR band, resulting in a low MNDWI values (Equation (2)). But at locations (points 3 and 4) close to Tapovan in downstream, there is an increase in the MNDWI values, which relate to the increase in the water level. This characteristic is properly witnessed in Srinagar as the MNDWI values increase at points 1–3 showing a sudden increase in the level of water as well as flooding of

Table 4. Coordinates of the point locations in Tapovan, Haridwar, Srinagar, and Bijnor.

	Tapovan	
Locations	Longitude	Latitude
1	79.73	30.41
2	79.73	30.47
3	79.69	30.49
4	79.63	30.49
	Srinagar	
Locations	Longitude	Latitude
1	78.87	30.25
2	78.84	30.24
3	78.79	30.23
4	78.76	30.22
	Haridwar	
Locations	Longitude	Latitude
1	78.31	30.12
2	78.29	30.08
3	78.26	30.03
4	78.23	29.98
	Bijnor	
Locations	Longitude	Latitude
1	78.05	29.46
2	78.05	29.44
3	78.04	29.38
4	78.09	29.33

nearby embankments. A decline was also witnessed at point 4 as it was taken in the canal, and after the event, the flood gates were closed so the water in the canal depleted. However, if we look at the other downstream regions of Haridwar and Bijnor, the MNDWI values does not change much (except for point 4 in Haridwar), which can be indicative of sediments clearing out because of travel distance of about 300 km from the Tapovan origin. At point 4, the water level decreased as a result of closure of the floodgates near Rishikesh, where the MNDWI values decrease. Locations in Bijnor indicates an increase in the flood plains at points 2 and 3 where the MNDWI increased from negative to positives values depicting the change in flood plain. Point 4 also witnessed intensive increase in water level as MNDWI values increased from 0.25 to 0.62 (Figure 5).

The chlorophyll index (NDCI) shows the change in chlorophyll concentrations in water. In Tapovan, the NDCI values decreased throughout the four locations due to the influx of debris into the river channel in the post-event. However, different instances of NDCI values were witnessed in the downstream regions of Srinagar, Haridwar, and Bijnor. In the case of Srinagar, NDCI levels increased at points 1, 2, and 3 could be due to transport of vegetation as debris (Figure 5). Most of the locations within Haridwar and Bijnor did not witness noticeable changes in the NDCI values due to distance of 300 km from Tapovan. However, the water quality reflected by the NDCI shows positive values depicting higher concentrations of chlorophyll due to the flow of vegetation. This might give mixed impressions if the role of NDCI is solely for assessing water quality and not accounting for debris as factor for water quality assessment after such a disaster. Similarly, as we look at the turbidity content (NDTI) in the river channels, throughout the four sections in downstream locations of Srinagar, Haridwar, and Bijnor, the turbidity level increased in the post-event image (Figures 2–4, 6) attributing to the addition of the sediment loads in the river water. However, close to the origin of Chamoli disaster at points 1 and 2, the NDTI values are low in the post-image. Accordingly, after the event, debris with

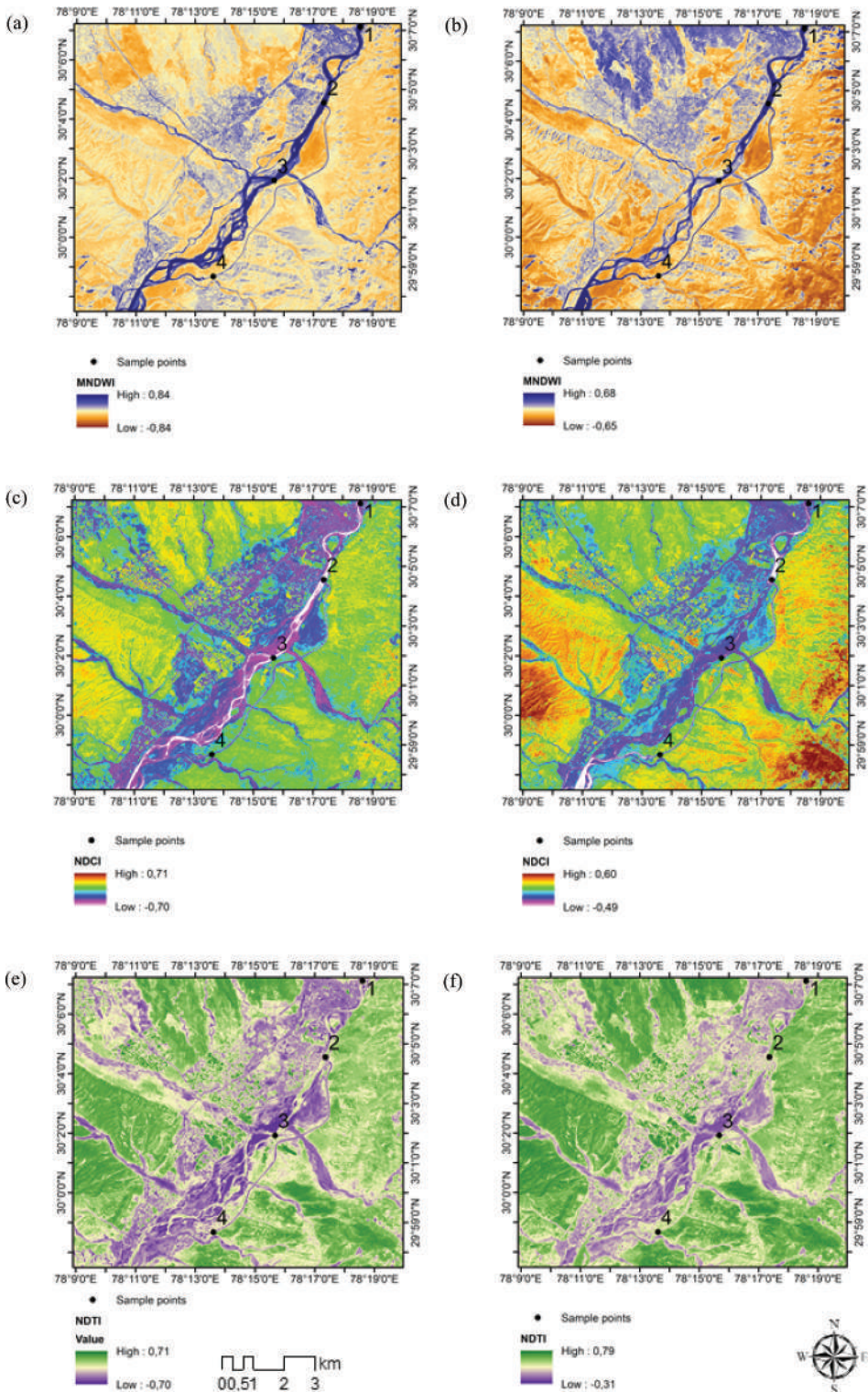


Figure 4. Changes in water quality indices at various locations for Haridwar (a, c, e: pre-event and b, d, f: post-event).



Figure 5. Changes in (a) MNDWI, (b) NDCI, and (c) NDTI for four locations (points 1–4) in Tapovan, Srinagar, Haridwar, and Bijnor.

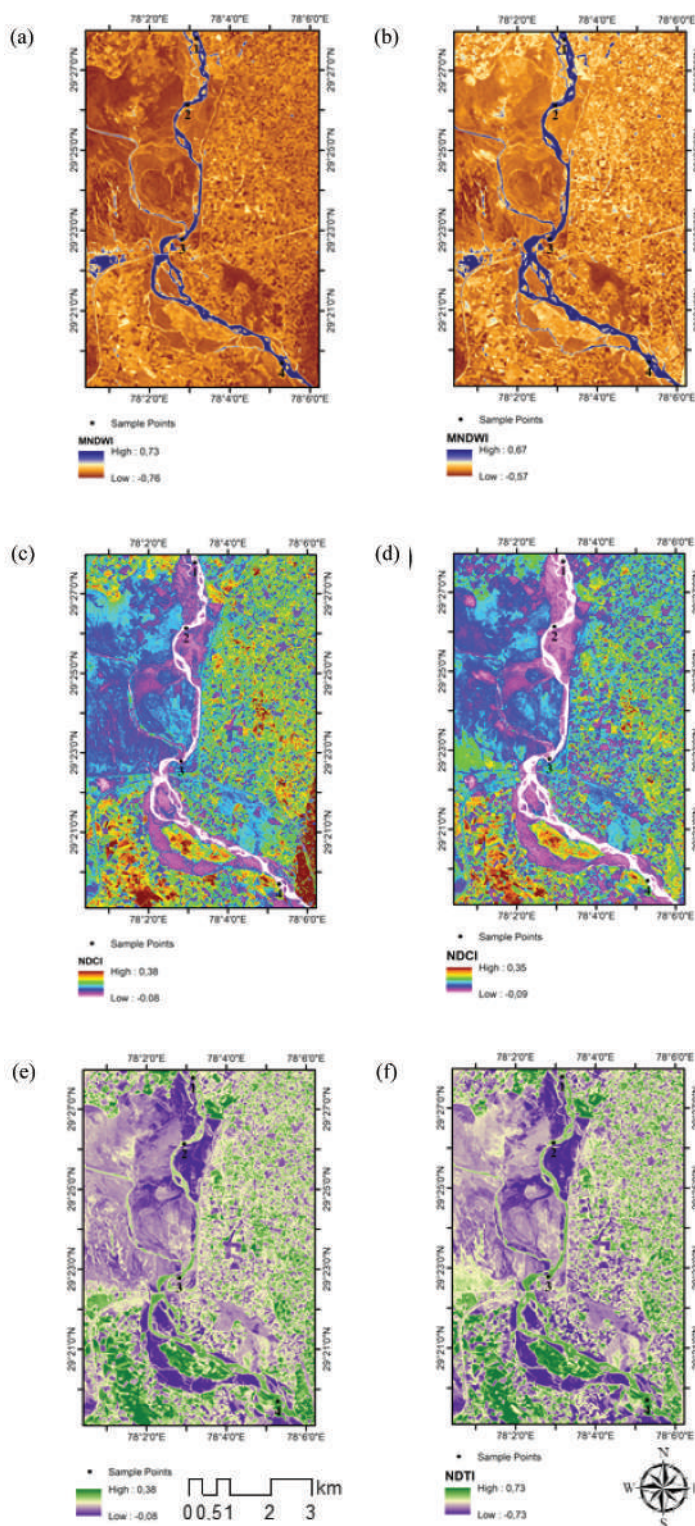


Figure 6. Changes in water quality indices at various locations for Bijnor (a, c, e: pre-event and b, d, f: post-event).

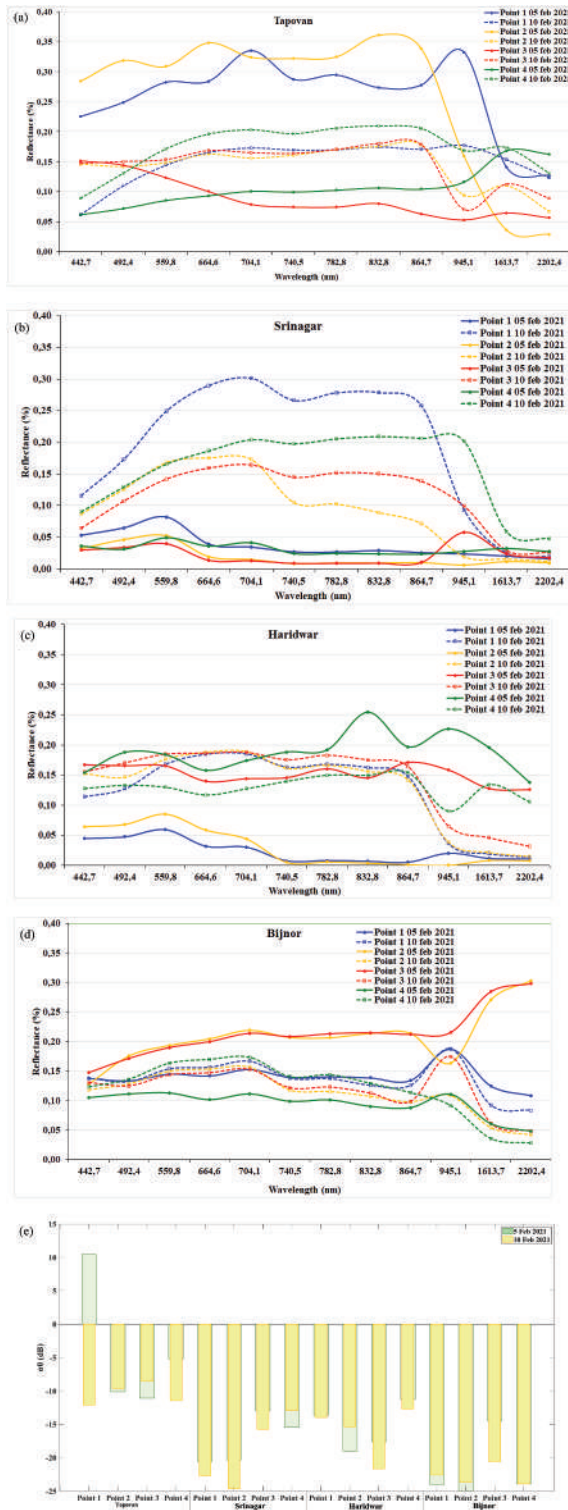


Figure 7. Changes in spectral signature in Tapovan (a), Srinagar (b), Haridwar (c), and Bijnor (d), and backscatter (e) in Sentinel-1 SAR data.

bare soil and glacial fragments deposited along the points 1 and 2, which led to a decrease in the surface reflectance of bands red and green. At points 3 and 4, which are further downstream near Rishi Ganga River, the NDTI values enhanced as in pre-event imagery, clear water can be seen and in post-imagery sediments concentration increased due to debris deposition into the river.

4.2. Changes in spectral reflectance in each band of Sentinel-2 and backscattering coefficients from Sentinel-1 SAR data

The effects of debris on the water quality can be comprehended straightforward when studying the changes in the spectral reflectance values and the backscatter coefficients. In [Figure 7](#), the solid (pre-event) and dotted (post event) lines show the surface reflectance values ([Figure 7](#)), respectively. At Tapovan (points 1 blue colour and 2 yellow colour), there is a sharp decrease in the reflectance values in the post-event snow-covered area, which indicates that debris from broken fragments from the glaciers and soil were transported in the river, showing low reflectance values. At points 3 and 4, the reflectance curves are higher in the post-event, which is attributed to influx of sediments into the river.

Similarly, at Srinagar, in the pre-event imagery, clear water can be seen in comparison to the post-event image where the surface reflectance at all the points increased due to the influx of debris ([Figure 7\(b\)](#)). Likewise, in Haridwar, points 1–3 show the same behaviour as Srinagar except in point 4, where the pre-event imagery shows higher surface reflectance compared to the post-event imagery. This could be due to the increase in the water level from the flooding of the Ganga River which absorbs most of the reflectance. Points 1 and 2 in Bijnor in the pre-event show higher surface reflectance as we considered points over sand bars which were later flooded in the post-event imagery ([Figure 7](#)) showing low reflectance values. Similarly, points 3 and 4 in the post-event have higher reflectance due to the increase in the flood plains.

Point 1 at Tapovan witnessed a sharp decrease in the backscatter values (10 decibels to -12 decibels), which indicates the steep terrain being flooded with debris and rock fragments, thus, reducing the backscatter information. The increase of backscatter signal from points 1 and 2 in Srinagar indicates the rise of water as backscatter values from water bodies show low values. Point 4 at Tapovan witnessed a decrease in the backscatter coefficient, relating to the increase in the flood water as water reflects less signal to the sensor, thus attributing lesser backscatter values. Similarly, the backscatter information from the other regions provides similar characteristics. Srinagar (points 1, 2, and 3), Haridwar (points 1, 3, and 4) and Bijnor (point 3) show decline in backscatter coefficient, indicating the rise of floodwater in the plains. At the same time, the other points have witnessed an increase in the backscatter, which can be related to presence of debris in the river channel.

5. Conclusions

In this study, we have studied the spectral reflectance characteristics of Sentinel-2 images to compute the water quality indices maps such as MNDWI, NDCI, and NDTI to evaluate the quality of water and changes in the flood plains over four study areas of Tapovan, Srinagar, Haridwar, and Bijnor, before and after the Chamoli disaster event. We also analysed the backscatter coefficient from Sentinel-1 data to study changes in water quality and flood plains along the Himalayan rivers. Changes were observed in the water flow from the source

(Tapovan) until the downstream location of Bijnor. The visual comparison of pre- and post maps clearly show increase in the sediment concentrations qualitatively in the rivers after the event. The sharp changes at the several locations clearly show the increase in the flood plains and water quality parameters. We attributed these changes to the increase in the water level after the Chamoli disaster, likely due to a slope failure and associated with the large volume of debris in the river.

Acknowledgements

The authors thank Google Earth Engine for their services and are also grateful to the Copernicus Programme for Sentinel-1 and -2 data sets. The authors are grateful to the anonymous referees for their useful comments/suggestions that have helped us to improve an earlier version of the manuscript.

Disclosure statement

No potential conflict of interest was reported by the author(s).

ORCID

Sansar Raj Meena  <http://orcid.org/0000-0001-6175-6491>

Kushanav Bhuyan  <http://orcid.org/0000-0002-6173-8696>

Akshansha Chauhan  <http://orcid.org/0000-0003-2668-2196>

Ramesh P. Singh  <http://orcid.org/0000-0001-6649-7767>

Data availability statement

The data that support the findings of this study are available from the corresponding author [Ramesh P. Singh rsingh@chapman.edu] upon reasonable request.

References

- Bhardwaj, A., R. J. Wasson, W. T. Chow, and A. D. Ziegler. 2021. "High-intensity Monsoon Rainfall Variability and Its Attributes: A Case Study for Upper Ganges Catchment in the Indian Himalaya during 1901–2013." *Natural Hazards* 105 (3): 2907–2936. doi:[10.1007/s11069-020-04431-9](https://doi.org/10.1007/s11069-020-04431-9).
- Bookhagen, B., and D. W. Burbank. 2010. "Toward a Complete Himalayan Hydrological Budget: Spatiotemporal Distribution of Snowmelt and Rainfall and Their Impact on River Discharge." *Journal of Geophysical Research: Earth Surface* 115 (F3). doi:[10.1029/2009JF001426](https://doi.org/10.1029/2009JF001426).
- Dash, P., R. P. Singh, and F. Voss. 2000. "Neotectonic Study of NW Himalaya Using Remote Sensing and GIS." *Current Science* 78: 1066–1070.
- Dwivedi, S., S. Mishra, and R. D. Tripathi. 2018. "Ganga Water Pollution: A Potential Health Threat to Inhabitants of Ganga Basin." *Environment International* 117: 327–338. doi:[10.1016/j.envint.2018.05.015](https://doi.org/10.1016/j.envint.2018.05.015).
- Fan, X., Q. Xu, C. J. van Westen, R. Huang, and R. Tang. 2017. "Characteristics and Classification of Landslide Dams Associated with the 2008 Wenchuan Earthquake." *Geoenvironmental Disasters* 4 (1): 12. doi:[10.1186/s40677-017-0079-8](https://doi.org/10.1186/s40677-017-0079-8).
- Gorelick, N., M. Hancher, M. Dixon, S. Ilyushchenko, D. Thau, and R. Moore. 2017. "Google Earth Engine: Planetary-scale Geospatial Analysis for Everyone." *Remote Sensing of Environment* 202: 18–27. doi:[10.1016/j.rse.2017.06.031](https://doi.org/10.1016/j.rse.2017.06.031).

- Gupta, S., N. Singh, D. Shukla, and R. P. Singh. 2019. "Morphological Mapping of 13 August 243 2017 Kotropi Landslide Using Images and Videos from Drone and Structure from Motion." *Earth and Space Science Open Archive* 244. doi:10.1002/essoar.10501438.1.
- Guyot, G. 1989. "Signatures spectrales des surfaces naturelles." *Téledétection satellitaire*, 5, Col. SAT, Ed. Paradigme, pp 178.
- Ives, J. 2004. *Himalayan Perceptions: Environmental Change and the Well-being of Mountain Peoples*. London: Routledge. doi:10.4324/9780203597569.
- Jupp, D.L.B., Kirk, J. T, O, and Harris, G.P. 1994. Detection, identification and mapping of Cyanobacteria using remote sensing to measure the optical quality of turbid inland waters. *Australian Journal of Marine and Freshwater Research*, 45 (5): 801–828. doi:10.1071/MF9940801.
- Kamboj, N., and V. Kamboj. 2019. "Water Quality Assessment Using Overall Index of Pollution in Riverbed-mining Area of Ganga-River Haridwar, India." *Water Science* 33 (1): 65–74. doi:10.1080/11104929.2019.1626631.
- Lacaux, J. P., Y. M. Tourre, C. Vignolles, J. A. Ndione, and M. Lafaye. 2007. "Classification of Ponds from High-spatial Resolution Remote Sensing: Application to Rift Valley Fever Epidemics in Senegal." *Remote Sensing of Environment* 106 (1): 66–74. doi:10.1016/j.rse.2006.07.012.
- McFeeters, S. K. 1996. "The Use of the Normalized Difference Water Index (NDWI) in the Delineation of Open Water Features." *International Journal of Remote Sensing* 17 (7): 1425–1432. doi:10.1080/01431169608948714.
- Meena, S., A. Chauhan, K. Bhuyan, and R. P. Singh. 2021a. "Impact of the Chamoli Disaster on Flood Plain and Water Quality along the Himalayan Rivers." In, *EGU General Assembly 2021: Copernicus Meetings*, pp EGU21–16592.
- Meena, S., K. Bhuyan, A. K. Chauhan, and R. P. Singh. 2021b. "Snow Covered with Dust after Chamoli Rockslide: Inference Based on High-resolution Satellite Data." *Journal: Remote Sensing Letters (TRSL)*. Article ID: TRSL 1931532. doi:10.1080/2150704X.2021.1931532
- Mishra, S., and D. R. Mishra. 2012. "Normalized Difference Chlorophyll Index: A Novel Model for Remote Estimation of Chlorophyll-A Concentration in Turbid Productive Waters." *Remote Sensing of Environment* 117: 394–406. doi:10.1016/j.rse.2011.10.016.
- Paul, M. J., R. Coffey, J. Stamp, and T. Johnson. 2019. "A Review of Water Quality Responses to Air Temperature and Precipitation Changes 1: Flow, Water Temperature, Saltwater Intrusion." *JAWRA Journal of the American Water Resources Association* 55 (4): 824–843. doi:10.1111/1752-1688.12710.
- Perrou, T., A. Garioud, and I. Parcharidis. 2018. "Use of Sentinel-1 Imagery for Flood Management in a Reservoir-regulated River Basin." *Frontiers of Earth Science* 12 (3): 506–520. doi:10.1007/s11707-018-0711-2.
- Peters, N. E., M. Meybeck, and D. V. Chapman. 2005. "Effects of Human Activities on Water Quality." *Encyclopedia of Hydrological Sciences*. doi:10.1002/0470848944.hsa096.
- Pradhan, B., R. P. Singh, and M. F. Buchroithner. 2006. "Estimation of Stress and Its Use in Evaluation of Landslide Prone Regions Using Remote Sensing Data." *Source: Natural Hazards And Oceanographic Processes From Satellite Data* 37 (4): 698–709.
- Ritchie, Jerry C., Paul V. Zimba, and James H. Everitt. 2003. "Remote sensing techniques to assess water quality." *Photogrammetric engineering & remote sensing*, 69(6): 695–704.
- Roback, K., M. K. Clark, A. J. West, D. Zekkos, G. Li, S. F. Gallen, D. Chamlagain, and J. W. Godt. 2018. "The Size, Distribution, and Mobility of Landslides Caused by the 2015 Mw7.8 Gorkha Earthquake, Nepal." *Geomorphology* 301: 121–138. doi:10.1016/j.geomorph.2017.01.030.
- Singh, R. P. 2005a. "Future Earthquakes and Other Natural Hazards: Impact on People Living in the Ganga Basin." *Current Science* 88 (7): 1025.
- Singh, R. P. 2005b. "Early Warning of Natural Hazards Using Satellite Remote Sensing." *Current Science* 89 (4): 592–593.
- Singha, M., J. Dong, S. Sarmah, N. You, Y. Zhou, G. Zhang, R. Doughty, and X. Xiao. 2020. "Identifying Floods and Flood-affected Paddy Rice Fields in Bangladesh Based on Sentinel-1 Imagery and Google Earth Engine." *ISPRS Journal of Photogrammetry and Remote Sensing* 166: 278–293. doi:10.1016/j.isprsjprs.2020.06.011.
- Solovey, T. 2019. "An Analysis of Flooding Coverage Using Remote Sensing within the Context of Risk Assessment." *Geologos* 25 (3): 241–248. doi:10.2478/logos-2019-0026.

- Stendardi, L., S. R. Karlsen, G. Niedrist, R. Gerdol, M. Zebisch, M. Rossi, and C. Notarnicola. 2019. "Exploiting Time Series of Sentinel-1 and Sentinel-2 Imagery to Detect Meadow Phenology in Mountain Regions." *Remote Sensing* 11 (5): 542. doi:[10.3390/rs11050542](https://doi.org/10.3390/rs11050542).
- Sun, R., D. An, W. Lu, Y. Shi, L. Wang, C. Zhang, P. Zhang, H. Qi, and Q. Wang. 2016. "Impacts of a Flash Flood on Drinking Water Quality: Case Study of Areas Most Affected by the 2012 Beijing Flood." *Heliyon* 2 (2): e00071. doi:[10.1016/j.heliyon.2016.e00071](https://doi.org/10.1016/j.heliyon.2016.e00071).
- Tahbildar, U. C., and R. P. Singh. 2005. "Hydro-electric Power Plant Projects in Northeastern India." *Current Science* 88 (6): 850.
- USEPA. 2008. "National Coastal Condition Report III," p. 329, Office of Research and Development/Office of Water. United States Environmental Protection Agency. EPA/842-R-08-002, Washington, DC 20460.
- Xu, H. 2006. "Modification of Normalised Difference Water Index (NDWI) to Enhance Open Water Features in Remotely Sensed Imagery." *International Journal of Remote Sensing* 27 (14): 3025–3033. doi:[10.1080/01431160600589179](https://doi.org/10.1080/01431160600589179).
- Ziegler, A. D., R. J. Wasson, A. Bhardwaj, Y. Sundriyal, S. Sati, N. Juyal, V. Nautiyal, P. Srivastava, J. Gillen, and U. Saklani. 2014. "Pilgrims, Progress, and the Political Economy of Disaster Preparedness—the Example of the 2013 Uttarakhand Flood and Kedarnath Disaster." *Hydrological Processes* 28 (24): 5985–5990. doi:[10.1002/hyp.10349](https://doi.org/10.1002/hyp.10349).